Organized flow from the South Pole to the Filchner-Ronne ice shelf: An assessment of balance velocities in interior East Antarctica using radio echo sounding data

Robert G. Bingham,[1,2] Martin J. Siegert,[1,3] Duncan A. Young,[4] and Donald D. Blankenship[4]

[1]   Ice flow through central Antarctica has the potential to transmit accumulation changes from deep-interior East Antarctica rapidly to the shelf, but it is poorly constrained owing to a dearth of ice-velocity observations. We use parameters derived from airborne radio echo sounding (RES) data to examine the onset, areal extent, and englacial conditions of an organized flow network (tributaries feeding an ice stream) draining from the South Pole to the Filchner-Ronne Ice Shelf. We classified RES flight tracks covering the region according to whether englacial stratigraphy was disrupted (i.e., internal layers diverged significantly from the surface and bed echoes) or undisrupted (i.e., internal layers closely parallel surface and basal topography), and we calculated subglacial roughness along basal reflectors. Where satellite-measured surface ice-flow speeds are available (covering 39% of the study region), regions of fast and tributary flow correspond with RES flight tracks that exhibit more disrupted internal layers and smoother subglacial topography than their counterparts in regions of slow flow. This suggests that disrupted internal layering and smooth subglacial topography identified from RES profiles can be treated as indicators of past or present enhanced-flow tributaries where neither satellite nor ground-based ice-flow measurements are available. We therefore use these RES-derived parameters to assess the balance-flux-modeled steady state flow regime between the South Pole and Filchner-Ronne Ice Shelf. The RES analysis confirms that an organized flow network drains a wide region around the South Pole into the Filchner-Ronne Ice Shelf. However, the spatial extent of this network, as delineated by the RES data, diverges from that predicted by currently available balance-flux models.

1.   Introduction

[2]   The identification and delineation of ice streams and their tributaries are critical to evaluating the form and flow of the major ice sheets, their long-term stability and their potential response to climate change and contribution to sea level. This is particularly so for the Antarctic Ice Sheet, which contains enough ice to raise global sea level by $60-70$ m [*Intergovernmental Panel on Climate Change*,

2001; *Hughes*, 1998], and where ice streams account for up to 80% of the total mass loss to the oceans each year [*Bennett*, 2003]. Since the early 1990s, the configuration of ice flow in Antarctica has been monitored extensively from space [*Bindschadler*, 1998], and the resultant observations have indicated that 'ice streams' (ice-flow speeds u typically ≥ 100 m yr^{-1}) drain relatively stable and inactive 'source regions' ($u \leq 5$ m yr^{-1}) via a complex system of 'tributaries' which represent a transitional flow regime ($5 \leq u \leq 100$ m yr^{-1}) [*Bamber et al.*, 2000; *Joughin et al.*, 1999]. In particular, recent observations have shown that tributaries can extend hundreds of kilometers into the ice sheet interior and may account for significant transfers of mass to the ice shelves and oceans from the deep interior of the ice sheet [*Berthier et al.*, 2003; *Joughin et al.*, 1999; *Lang et al.*, 2004]. However, at present satellite coverage over Antarctica is incomplete, such that while organized flow networks (i.e., ice streams and tributaries) are relatively well constrained in some regions [*Alley and Bindschadler*, 2001], ice

[1]Centre for Polar Observation and Modelling, Bristol Glaciology Centre, School of Geographical Sciences, University of Bristol, Bristol, UK.
[2]Now at British Antarctic Survey, Natural Environment Research Council, Cambridge, UK.
[3]Now at Centre for Polar Observation and Modelling, School of GeoSciences, University of Edinburgh, Edinburgh, UK.
[4]Institute for Geophysics, John A. and Katherine G. Jackson School of Geosciences, University of Texas at Austin, Austin, Texas, USA.

flow through many parts of Antarctica, particularly the deep interior of the ice sheet, remains enigmatic.

[3] The ice-flow field between the South Pole (SP) and the Filchner-Ronne Ice Shelf (FRIS) remains especially poorly constrained by current observations [*Rignot and Thomas*, 2002]. This is because much of the region lies south of 87°S, the current latitudinal limit of satellite remote sensing observations of ice surface velocities. North of this limit, satellite observations detail enhanced/fast ice flow along the Foundation Ice Stream (FIS) and the downstream trunk of the Support Force Ice Stream (SFIS) (Figure 1). Crucially, however, the onset region of the SFIS, which may lie deep within the interior of the East Antarctic Ice Sheet, and thus may act as a significant corridor for ice transport from the interior to the shelf, has not been delineated by empirical evidence.

[4] South of 87°S, we presently rely on balance-flux modeling [*Budd and Warner*, 1996] to estimate ice-flow fields, and recently produced maps of depth-averaged steady state balance velocities, which imply the existence of organized flow networks throughout both West and East Antarctica [*Bamber et al.*, 2000; *Wu and Jezek*, 2004], highlight a distinct organized flow network constituting at least one tributary draining from the vicinity of the SP, into the SFIS, and thereon into the FRIS (Figure 1). However, although balance velocities are often treated as proxies for ice flow, their derivation is primarily dependent upon the availability and quality of surface elevation data, which is severely restricted south of 86°S, the southerly limit of IceSAT [*Bamber and Gomez-Dans*, 2005]. Balance velocities are secondarily a function of ice thickness and surface mass balance, which are additionally more sparse over the SP region than in most other regions of Antarctica [*Davis et al.*, 2005; *Lythe et al.*, 2001]. Balance velocities over central Antarctica can therefore be treated only as rough approximations of ice flow, and there has to date been no empirical confirmation of the existence, or otherwise, of the balance-flux-modeled organized flow network draining from the vicinity of the SP into the SFIS, potentially connecting the deep interior of the East Antarctic Ice Sheet to the FRIS. This paper addresses that issue, and assesses the validity of balance fluxes south of 86°S, through the use of airborne ice-penetrating radio echo sounding (RES) data to identify and constrain the englacial/subglacial configuration of organized flow between the SP and the FRIS.

[5] RES has been used previously in two ways to determine the distribution of ice streams and tributaries elsewhere in Antarctica. First, englacial stratigraphy demonstrably varies with flow regime such that internal layers, commonly taken as isochrones [*Eisen et al.*, 2003; *Miners et al.*, 2002], are relatively flat, parallel the surface and bed, and may be spatially continuous over distances of several hundred km in regions of stable or very slow flow (<5 m yr^{-1}), but can become highly disrupted or buckled in association with flow contrasts across ice stream margins and within tributaries. These internal layering characteristics have been used, for example, to delineate the spatial extent and stability of the Bindschadler Ice Stream (formerly Ice Stream D), West Antarctica [*Siegert et al.*, 2003], and to investigate the spatial distribution of organized flow in Wilkes Land, East Antarctica [*Rippin et al.*, 2003b]. Secondly, it has recently been established that the spectral roughness of subglacial topography can be diagnostic of ice flow conditions [*Hubbard et al.*, 2000] such that ice streams are typically underlain by smoother topography than surrounding, slower-flowing ice ridges and source regions [*Siegert et al.*, 2005, 2004; *Taylor et al.*, 2004]. In this paper, we analyze englacial stratigraphy and subglacial roughness within existing RES data sets collected between the SP and FRIS to examine the onset, areal extent and englacial conditions of a potential organized flow network draining from interior East Antarctica to the FRIS via the Support Force drainage basin.

2. Methods

2.1. Study Domain and Existing Flow-Velocity Grids

[6] We focus on a 1010 km × 920 km region of Antarctica containing the South Pole (SP), the Support Force Ice Stream (SFIS), and associated tributaries, as modeled by balance velocities [*Bamber et al.*, 2000; *Wu and Jezek*, 2004] (Figure 1). The study domain also incorporates much of the neighboring Foundation Ice Stream (FIS) drainage basin (Figure 1). To describe the orientations of geographical features within the study domain surrounding the South Pole we adopt the Scientific Committee for Antarctic Research standard nomenclature whereby Grid N, Grid S, Grid W, and Grid E follow the 0°, 180°, 90°W and 90°E meridians respectively.

[7] A surface-velocity grid at 1 km resolution has been derived using both conventional interferometry and speckle-tracking techniques over 39% of the study region, incorporating almost all of the FIS [*Joughin et al.*, 2006] (Figure 1). In areas without satellite-derived surface-velocity coverage, balance velocities presently act as proxies for ice flow (Figure 1). The balance velocity grid used here [*Le Brocq et al.*, 2006] builds on those of *Bamber et al.* [2000] and *Wu and Jezek* [2004], using the *Budd and Warner* [1996] algorithm at 5 km^2 resolution but adopting the driving stress, rather than the surface, to route the flow. Key input data sets were the RAMP surface DEM [*Liu et al.*, 1999], ice thicknesses from BEDMAP [*Lythe et al.*, 2001], and snow accumulation rates from *Vaughan et al.* [1999]. The final balance velocity grid was smoothed using a filter whose size varies with ice thickness; thus longitudinal stresses, hence flow vectors, are scaled to ice thickness. Velocity was not calculated where ice thickness <50 m. We keep in mind that in this region of central Antarctica the data sets used to derive the balance velocities are of inconsistent availability and quality [*Liu et al.*, 1999; *Lythe et al.*, 2001; *Vaughan et al.*, 1999]. Hence we consider balance velocities in the context that (1) they currently represent the *only* guide to ice velocities through much of the region but (2) it is important to test whether they correspond with additional data sets which provide information about ice flow. Within the study domain the match between the available satellite-derived surface velocities and the *Le Brocq et al.* [2006] balance velocity grid is good (Figure 1). Later in the paper we consider the correspondence between balance velocities and RES data sets that manifest variations in ice flow.

[8] For subsequent comparisons with our RES findings, we consider results both over the entire 9.3 × 10^5 km^2 domain and a subset of the region comprising the 3.6 × 10^5 km^2 covered by satellite-derived surface-velocity obser-
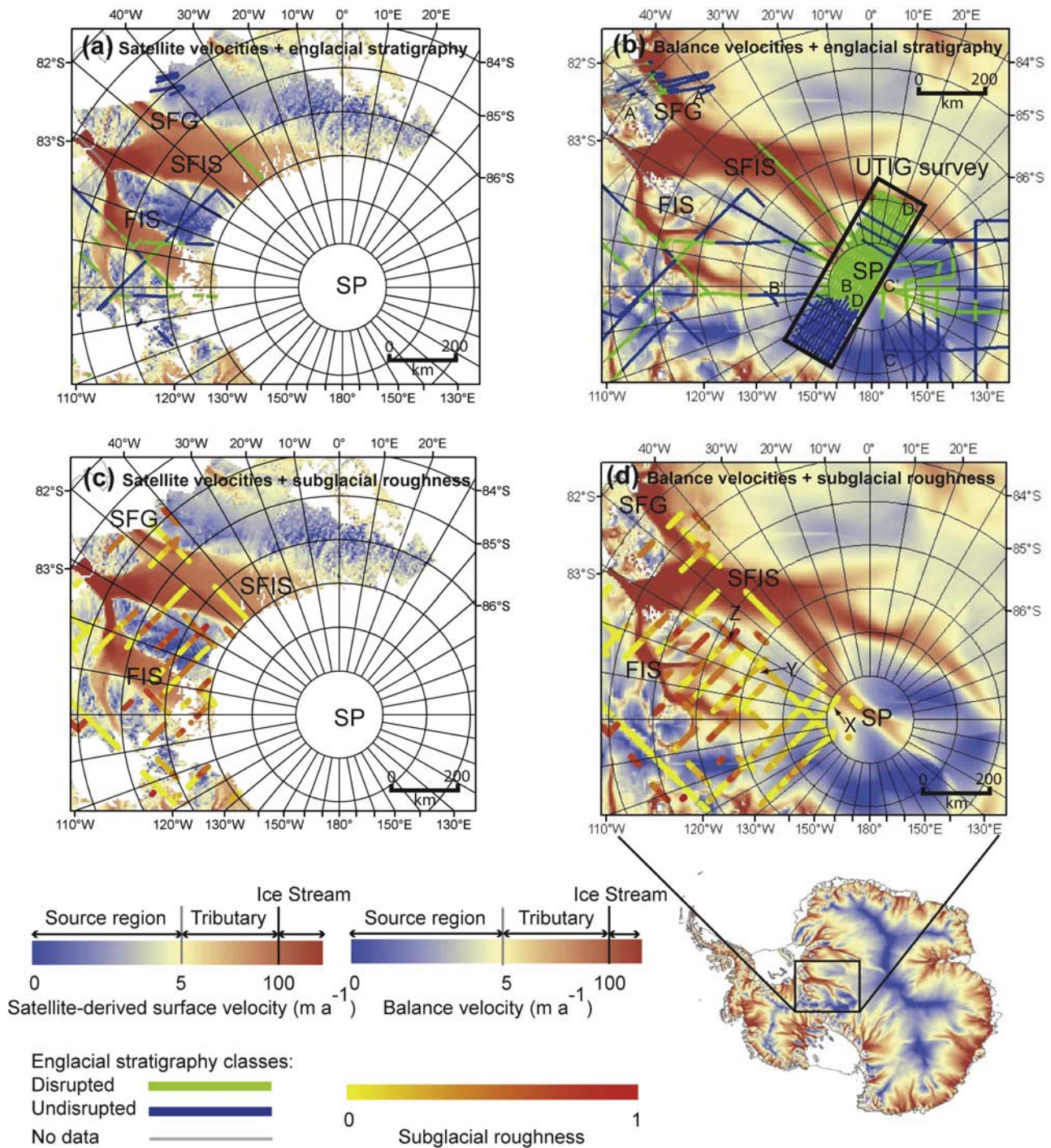
Figure 1. Inset: Depth-averaged balance velocities over Antarctica after *Le Brocq et al.* [2006], showing the location of the study area and highlighting the potential significance of Support Force Ice Stream in connecting the South Pole to Filchner-Ronne Ice Shelf. Classification of englacial stratigraphic variations superimposed over (a) available satellite-derived surface velocities and (b) depth-averaged balance velocities. In Figure 1b the UTIG data set is shown in the boxed region, and the locations of selected RES profiles given in Figure 2 are indicated. In our analysis, we divide both velocity data sets into regions of slow (source region) flow (<5 m yr^{-1}), intermediate (tributary) flow (5−100 m yr^{-1}), and fast (ice stream) flow (>100 m yr^{-1}) (see text). (c, d) Variations in subglacial roughness superimposed over velocity distributions as in Figures 1a and 1b. Roughness values are plotted at the midpoints of 70 km analysis windows, and have extremes of 0 (a perfectly flat bed) and 1 (a bed whose vertical and horizontal undulations match, i.e., maximum roughness). In Figure 1d, sites X, Y, and Z refer to examples of roughness derivations shown in Figure 3. Other abbreviations refer to the following locations: FIS (Foundation Ice Stream), SFG (Support Force Glacier), SFIS (Support Force Ice Stream), and SP (South Pole).

vations. Within this "control zone", we assume that satellite-derived surface ice-flow fields constitute a good representation of the depth-averaged ice-flow fields, and hence should provide a reasonable match with flow fields derived using RES methods. Here we use satellite-derived surface velocities, u, to define regions of slow (<5 m yr^{-1}), intermediate ($5-100$ m yr^{-1}) and fast (>100 m yr^{-1}) flow (Figure 1), designed broadly to correspond with flow conditions in interior source regions, tributaries and ice stream margins, and ice streams respectively. This categorization of the ice-flow speed data is necessary to facilitate comparisons with the analysis of the categorized RES data (discussed below), but we stress that the flow speeds of 5 and 100 m yr^{-1} merely represent markers along a continuum from interior source region flow through tributary flow through fast (ice streaming) flow. The values were chosen based upon frequent statements that ice streams flow >100 m yr^{-1} [*Bamber et al.*, 2000; *Joughin et al.*, 1999] and interior source regions typically experience flow of <5 m yr^{-1} [*Bennett*, 2003; *Rippin et al.*, 2003a].

[9] For further comparison with the RES findings, we similarly partition the entire study area into regions of slow, intermediate and fast flow, but in this case using modeled depth-averaged balance velocities, v, as the basis for defining the flow fields (Figure 1). In this case we consider the derived flow fields only as loose proxies, rather than reliable representations, of differences in ice flow throughout the study domain, whose accuracy may be verified, or otherwise, by comparison with the empirical evidence of the ice-flow configuration derived from analyzing RES data. Finally, we also compare our RES analysis with ice thickness data from the BEDMAP database [*Lythe et al.*, 2001].

2.2. RES Data Collection

[10] We utilize two RES data sets in our analysis. The first is derived from an extensive airborne survey conducted over much of the Antarctic Ice Sheet between 1971 and 1979 by a consortium of the U.K. Scott Polar Research Institute, the U.S. National Science Foundation and the Technical University of Denmark (SPRI-NSF-TUD data set). The second is derived from a University of Texas Institute for Geophysics aerogeophysical survey conducted between 1997 and 1998 over a region extending from the Transantarctic Mountains to 220 km past the SP along the 150°W/30°E meridians (UTIG data set).

[11] The SPRI-NSF-TUD data were collected with a 250 ns 60 MHz pulse RES system, and were recorded in two formats. "Z-scope" radargrams, analogue records which display two-way electromagnetic travel times plotted against real time, were produced from sampling several times per second, yielding pseudo cross sections of the englacial stratigraphy of the ice sheet in which numerous internal layers are often present (e.g., Figures 2a–2c). "A-scope" records, binary files which detail two-way travel times versus signal strength with associated navigational fixes, were produced from sampling every 15 s (equating to $\sim0.7-1.5$ km), and were primarily designed to locate the bed and construct maps of bed depth and ice thickness [*Drewry*, 1983; *Lythe et al.*, 2001]. A bed reflector was located along 86% of the flight tracks, and the accuracy of the navigational fixes, also used for tying in the Z-scope data, is generally stated to be <5 km but is typically <1 km

[*Drewry*, 1983; *Rose*, 1978, 1979; *Siegert*, 1999]. Along some sections of flight track, owing to occasional equipment failure, only one type of record, either A-scope or Z-scope, was recorded, precluding the analysis of englacial stratigraphy (which uses Z-scopes) and/or subglacial roughness (which uses A-scopes) along the affected stretches of flight track respectively. Despite dating back ~30 years, correspondence of these data with modern data sets elsewhere in Antarctica has confirmed their overall excellent quality and comparability [*Siegert et al.*, 2004].

[12] The radar transmitter used for the modern (1997–1998) UTIG survey was similar to that used for the SPRI-NSF-TUD survey. However, data acquisition was achieved digitally, and records equivalent in nature to the SPRI-NSF-TUD A-scopes described above were collected at 5 Hz, yielding radargrams with horizontal sampling of ~12 m (e.g., Figure 2d). Navigation and positioning for the UTIG survey were undertaken using dual-carrier wave GPS with an accuracy of 20 cm [*Davis*, 2001]. Although the UTIG radargrams therefore reflect a greater sampling frequency than the SPRI-NSF-TUD radargrams, internal layers are easily trackable in both sets of radargrams, and major differences in the nature of internal layers that could be attributed to variations in sampling frequency were not observed when comparing between the two sets of records.

2.3. Analysis of Englacial Stratigraphy

[13] All RES data lying within the study domain were classified according to whether internal layers displayed in their radargrams (e.g., Figure 2) are (1) "undisrupted," (2) "disrupted," or (3) "absent" [*Rippin et al.*, 2003b; *Siegert et al.*, 2003]. Internal layering along RES flight tracks was identified as "undisrupted" where numerous internal layers are easily identifiable and relatively flat over large distances, the amplitudes of all undulations are lower than those of the bed, and the dominant wavelengths of internal layers and the bed are similar. RES flight tracks were labeled as "disrupted" where internal layers diverge significantly from subglacial topography, the amplitudes of all undulations significantly exceed those of the bed, and the wavelengths of internal layers are much lower than those of the bed. Internal layering was deemed "absent" where clear layering (either undisrupted or disrupted) is not visible in a given profile. The absence of internal layering in RES profiles may reflect genuine physical phenomena such as the destruction or interspersion of internal layers due to prolonged and extensive buckling or warping, or signal scattering over a large crevasse field, both of which are indicative of fast flow. Alternatively, however, lack of visible internal layering may own to nonglaciological phenomena such as a loss of radio wave power during data collection, perhaps owing to increasing ice thickness or aircraft altitude, or problems with the RES unit's power source [*Rose*, 1978]. For this reason, we do not interpret flow dynamics from flight tracks with no internal layering.

2.4. Analysis of Subglacial Roughness

[14] Subglacial roughness, the variation of bed elevation with horizontal distance, was evaluated on the SPRI-NSF-TUD lines directly following methods described by *Taylor et al.* [2004]. Consistent with previous derivations of regional subglacial roughness elsewhere in Antarctica
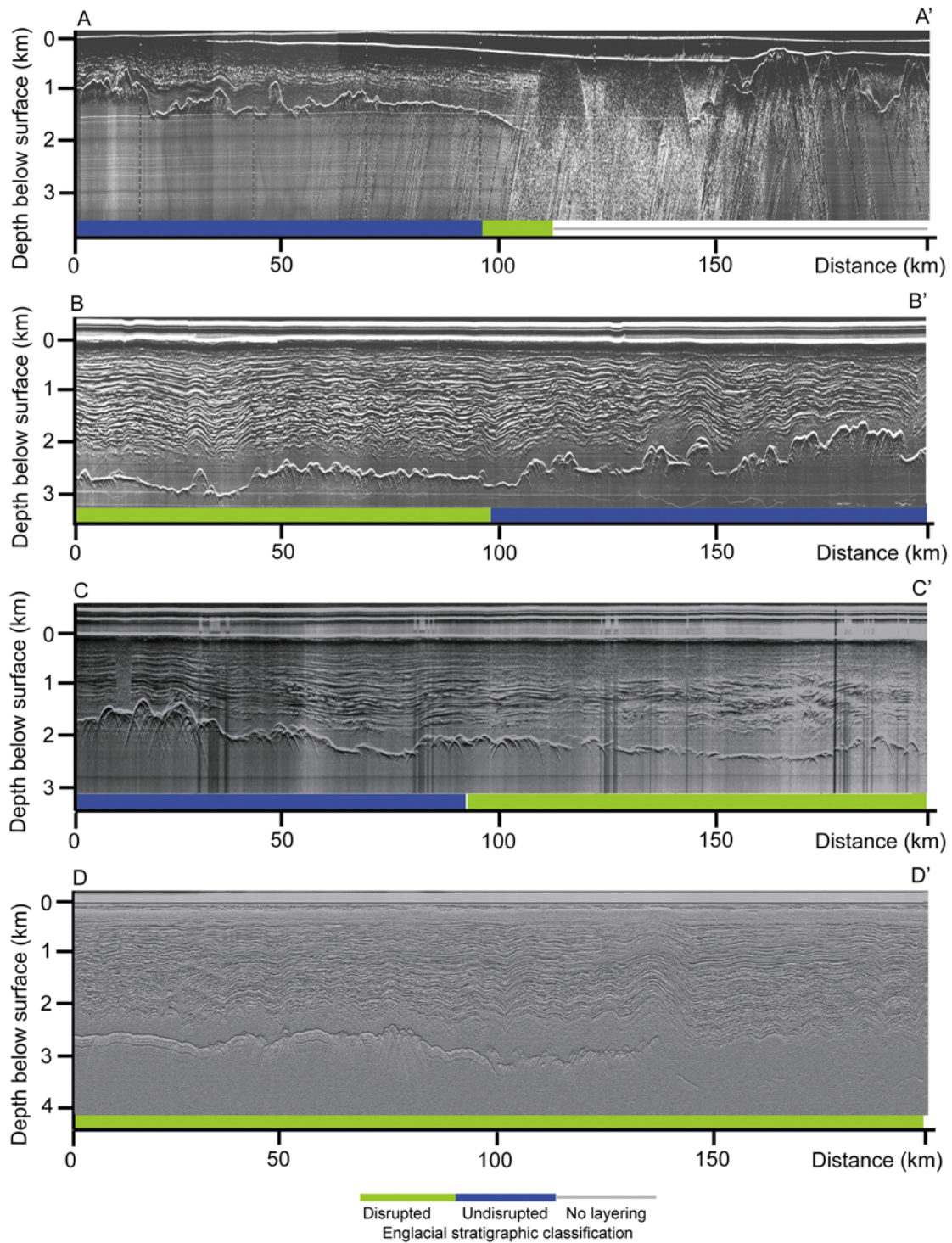
Figure 2. Selected RES profiles analyzed for englacial stratigraphic disruption, shaded along distance axis according to assigned class. (a) Line 031 from the 1978/79 SPRI-NSF-TUD survey, showing sections with undisrupted, disrupted and no visible internal layers. (b) Line 112 from the 1974/75 SPRI-NSF-TUD survey, showing the transition from disrupted to undisrupted layering. (c) Line 121 from the 1974/75 SPRI-NSF-TUD survey, showing the transition from undisrupted to disrupted layering. (d) Line PPT/Ey/Y02a from the 1997/1998 UTIG survey, showing widespread buckling crossing the South Pole along the 150°W/30°E meridians. Profile locations are supplied in Figure 1b.

[*Siegert et al.*, 2005, 2004], data preparation comprised splitting RES flightlines into components approximately orthogonal and parallel to ice flow, and discarding flight-lines which are neither. Subglacial roughness power spectra were then determined over a moving 70 km window along each flightline over which a forward Fast Fourier Transform (FFT) was performed. 70 km represents the minimum length over which the FFT could be calculated given that
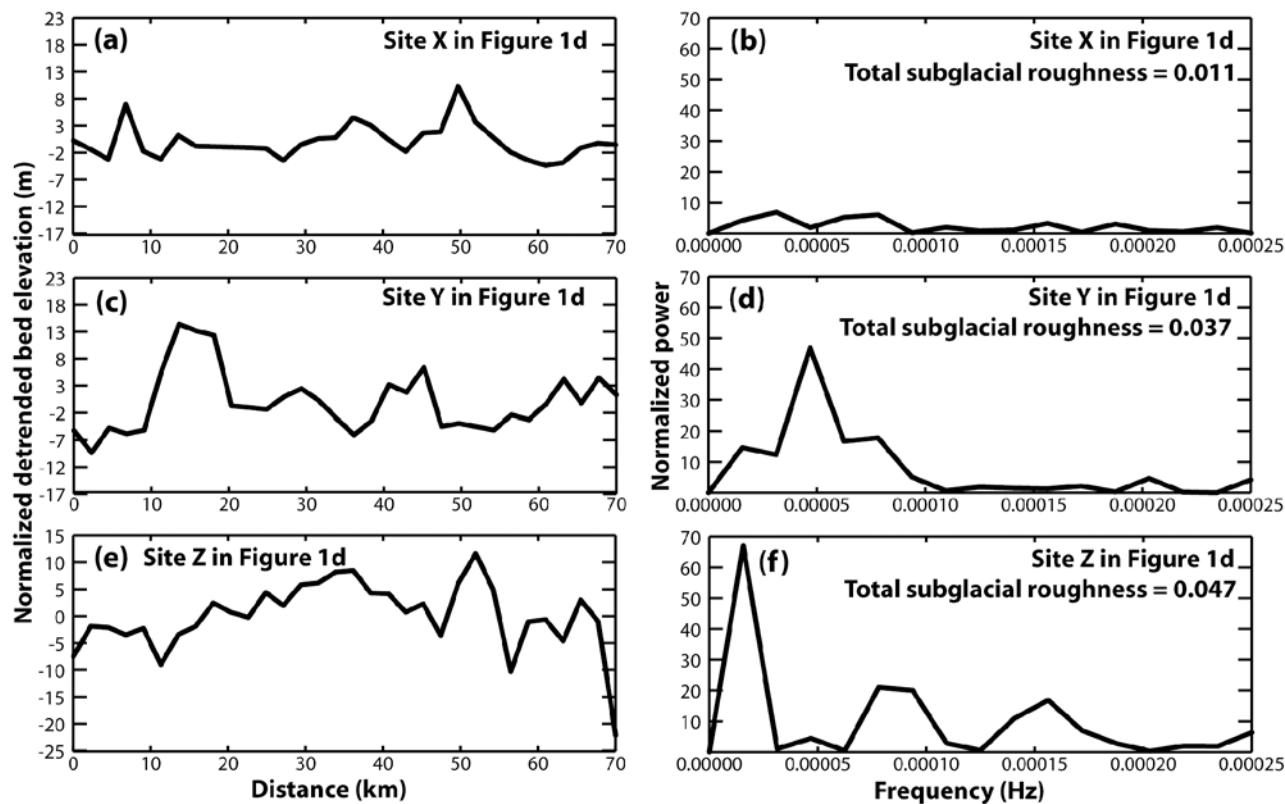
Figure 3. Examples of bed returns and power spectra used to generate total subglacial roughness values. (a) Normalized detrended bed elevation and (b) spectral power density plot for Site X (marked on Figure 2d). Total subglacial roughness is calculated from the area beneath the curve and is smoother than in the other two profiles given here as examples. (c) Normalized detrended bed elevation and (d) spectral power density plot for Site Y (marked on Figure 2d). (e) Normalized detrended bed elevation and (f) spectral power density plot for Site Z (marked on Figure 2d). This site has the roughest subglacial topography of the three examples.

each FFT requires 2^N datapoints, a suggested minimum value for N is 5 [*Brigham*, 1988] and the maximum distance between two soundings is 2.19 km. Hence lines <70 km in length were removed during preprocessing. A further prerequisite for using the FFT technique is that continuous data are required along each section of flight track analyzed. Most of the flight tracks we analyzed are continuous but for occasional gaps of 2−3 datapoints which, if not interpolated, would preclude FFT analysis. We therefore interpolated linearly over minor (<7 km) gaps in otherwise continuous raw bed returns. Of the 2422 datapoints thus analyzed for subglacial roughness in this study, 176 (<10%) were interpolated and 95% of these were interpolated over gaps <5 km.

[15] Following *Taylor et al.* [2004] the FFT power spectra were detrended linearly using least squares regression to remove the dominance of very long wavelength (>35 km) roughness, and amplitude was normalized with respect to N. This yields roughness power spectra which are dimensionless in the y (vertical) direction, and whose frequencies (x, horizontal coordinate) are represented as fractions of the analysis-window length, hence lie between 0 and 1. Total subglacial roughness (plotted at the midpoint of each 70 km analysis window; Figures 1c and 1d) is defined as the integral of the FFT spectral power density plot for each

roughness analysis window. Some examples of the spectral power density plots are provided in Figure 3. Essentially, a subglacial roughness of 0 represents a perfectly smooth bed, with no vertical undulations. Subglacial roughness values increasing from 0 reflect an increasing number of vertical undulations in the bed, with the reciprocal of the subglacial roughness value yielding the characteristic wavelength over which these undulations are observed.

3. Results

3.1. Englacial Stratigraphy

[16] Figures 1a and 1b show the RES flight tracks analyzed for disruption to englacial stratigraphy in this study, shaded according to whether internal layering is undisrupted, disrupted, or absent. The classified flight tracks are superimposed onto the available satellite-derived surface velocities (Figure 1a) and the depth-averaged balance velocity plot discussed above (Figure 1b). Selected examples of the analyzed RES profiles, illustrating sections of undisrupted, disrupted and absent layering, and transitions between these categories, are given in Figure 2. Overall, englacial stratigraphy was classified over 18,130 km of flight tracks, 20% of which lie within the 39% of the domain constrained by satellite velocity measurements. Over the entire study domain, incorporating the FIS, SFIS

Table 1. Breakdown of Internal Layering Characteristics Over the Satellite-Constrained Control Zone and the Entire Support Force/Foundation Ice Stream Domain

	Control Zone, 3.9×10^5 km^2 Area	Entire Domain, 9.3×10^5 km^2 Area		
	SPRI Database[a]	SPRI Database[a]	UTIG Database	Combined Database
Track length with visible internal layers, km	1780	7640	6600	14240
Track length with well-preserved layers, km	1050	3960	2610	6570
Track length with buckled internal layers, km	730	3680	4000	7680
Track length with no visible internal layers, km	1770	3890	0	3890
Totals, km	3550	11530	6600	18130

[a]SPRI-NSF-TUD database is abbreviated to "SPRI."

and the SP, internal layering is visible along 79% (14,240 km) of the flight tracks and, where it is visible, 46% of RES profiles contain undisrupted internal layering and the remaining 54% comprise disrupted internal layering. Within the satellite-constrained control zone, internal layering is visible along 50% (1780 km) of flight tracks, and is undisrupted in 59% of cases and disrupted for the remaining 41%. The full breakdown of internal layering characteristics derived from the SPRI-NSF-TUD and UTIG data sets is provided in Table 1.

[17] Consistent with RES observations across the Siple Coast [*Siegert et al.*, 2004] and East Antarctica [*Rippin et al.*, 2003b], wherever disruption (or buckling/warping) of internal layering was identified the disrupted layers occur at depth and are typically overlain by continuous layering in the upper depth quartile (e.g., Figure 2). The features are therefore similar in appearance to the zones of high scattering found in East Antarctica described by *Matsuoka et al.* [2003, 2004]. Over the control zone, flight tracks in which disrupted layers exist are clearly associated with the FIS and its associated tributaries, in addition to the northerly trunk of the SFIS (Figure 1a). Statistical observations on mean ice thicknesses and ice-flow velocities demonstrate that flight tracks with disrupted internal layering occur where ice thickness is 28% greater and satellite-derived surface velocity, u, is 437% greater, than along flight tracks with undisrupted internal layering (Table 2). Within the control zone, depth-averaged balance velocities, v, are also faster where internal layers are disrupted, 157% greater than in regions with undisrupted layers (Table 2). Outside the control zone, internal layering surrounding much of the SP vicinity is clearly disrupted, but the disruption is more broadly distributed across the SP region than is suggested by balance-velocity modeling, which instead indicates only a narrow 'finger' of tributary flow crossing the SP (Figure 1b). Layer disruption is also observed along the eastern margin of SFG, although most lines crossing the SFG exhibit no visible internal layers (Figures 1b and 2a). Over the study domain as a whole, disrupted internal layering occurs on average where ice is 17% thicker, and v is 89% faster, than areas where undisrupted layering is identified.

[18] Examining the variations in englacial stratigraphy with respect to regions of slow (<5 m yr^{-1}), intermediate (5−100 m yr^{-1}) and fast (>100 m yr^{-1}) u and/or v (Table 3), it is notable that disruption of internal layering is mostly associated with regions of intermediate or fast flow, while more often than not preservation of internal layering is associated with slow flow. Within the satellite-constrained region, a striking majority (88%) of flight tracks with disrupted internal layering occur where u is intermediate or fast, while the majority (53%) of flight tracks with undisrupted internal layering occur where u is slow. Within this same region, 81% of disrupted internal layers coincide with intermediate/fast v, while 38% of undisrupted internal layers are associated with slow v. Over the entire domain, 52% of disrupted internal layers occur where v is intermediate/fast, while 78% of undisrupted internal layers correspond with slow v. These patterns can also be observed with reference to histograms showing the frequency of disrupted/undisrupted datapoints in relation to u and/or v (Figure 4). The frequency of datapoints with undisrupted internal layering drops exponentially in relation to increasing flow speeds, while the frequency of datapoints with disrupted internal layering is less variable with respect to ice flow speeds (Figure 4). The relative effect is that with increasing flow speeds increasing proportions of flight tracks exhibit disrupted internal layering rather than undisrupted internal layering.

3.2. Subglacial Roughness

[19] Figures 1c and 1d show the RES flight tracks analyzed for subglacial roughness in this study, again superimposed over the satellite and balance velocity data respectively. Approximately 4160 km of flight tracks were analyzed for subglacial roughness within the study domain, 38% of which are approximately parallel to ice flow and 62% of which are orthogonal to ice flow. 56% (2340 km) of these flight tracks lie within the satellite-constrained region, 41% parallel to, and 59% orthogonal to, the predominant surface ice-flow direction. Over the study domain as a whole, subglacial roughness values are highly variable (mean 0.102; range 0.0−0.902).

[20] Over the control zone, there is a clear correspondence between the distribution of subglacial roughness values and the ice flow configuration as defined by satellite analysis (Figure 1c). Thus flight tracks with low subglacial roughness cross the FIS and the lower section of the SFIS, whereas higher roughness values are observed elsewhere, notably over the Pescora Escarpment between FIS and

Table 2. Comparison of Internal Layering Characteristics With Ice Thickness, Satellite-Derived Surface Velocity, and Depth-Averaged Balance Velocity Over the Control Zone and Entire Study Region

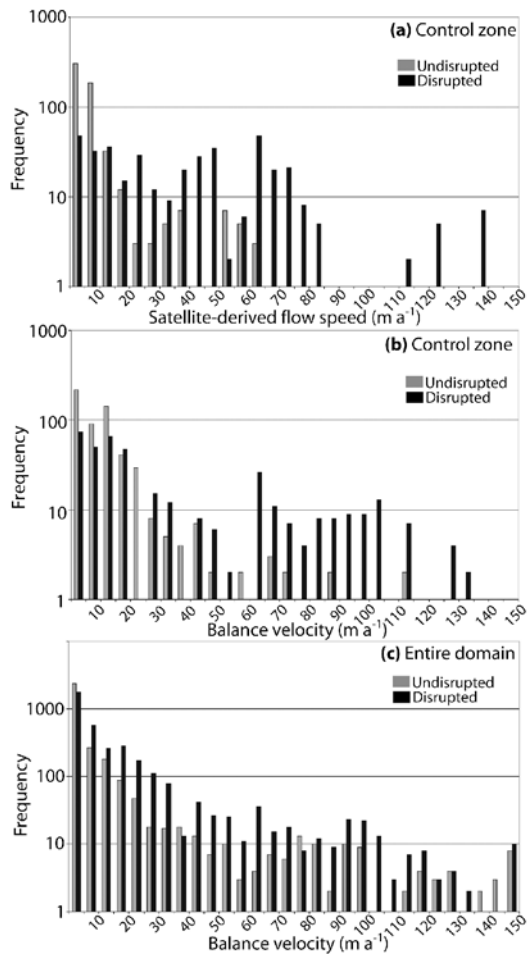|	Control Zone		Entire Domain	
	Undisrupted[a]	Disrupted[a]	Undisrupted[a]	Disrupted[a]
Mean ice thickness, m	1390	1780	2280	2660
Mean InSAR surface velocity, m yr^{-1}	7.5	40.3	–	–
Mean balance velocity, m yr^{-1}	13.6	35.0	8.0	15.1

[a]Layer class.

Figure 4. Histograms of internal layering characteristics versus ice flow speeds. Datapoints along each RES flight track were characterized as exhibiting primarily undisrupted (gray columns) or disrupted (black columns) internal layering, and are here plotted against (a) satellite-derived ice-flow speeds, only available in the control zone; (b) balance velocities only in the control zone; and (c) balance velocities across the entire study domain. In all three cases, disrupted internal layering predominates over undisrupted layering at higher ice-flow speeds.

SFIS. Indeed, over the satellite-constrained region subglacial topography is roughest where u is slow, approximately half as rough where u is intermediate, and approximately half as rough again where u is fast (Table 4). The same, but

not as striking, pattern is observed when comparing subglacial roughness values with balance velocities over the control zone: subglacial topography is roughest where v is slow, 17% smoother where v is intermediate, and 18% smoother again where v is fast (Table 4).

[21] Outside the control zone, low subglacial roughness values are observed widely across the region lying between longitudes 55°W–125°W and latitudes 88°S–89°S, an area which balance velocity modeling currently suggests is characterized by slow flow (Figure 1d). However, this is a region in which disrupted internal layering is widely observed (Figure 1b). Low subglacial roughness is also observed over SFG, neighboring the Pensacola Mountains. However, over the study domain as a whole, the correspondence between subglacial roughness and balance velocities is not as clear as that observed within the satellite-constrained region. Here, compared with subglacial roughness where v is slow, subglacial topography is actually 14% rougher where v is intermediate but 4% smoother where v is fast (Table 4).

[22] Scatterplots of subglacial roughness versus ice flow speed (represented by u and/or v) (Figure 5) back up these statements. Regardless of whether roughness is analyzed on flight tracks parallel or orthogonal to the principal ice-flow direction, smoother subglacial topography is typically observed where ice-flow speeds are faster (Figure 5). The relationship between fast flow and a smooth bed is clearest where comparing subglacial roughness with satellite-derived flow speeds (Figure 5a); this is expected given that satellite measurements give a more accurate picture of ice flow speeds than balance velocities can provide in areas of poor data coverage.

4. Discussion

[23] In the control region of our analysis (i.e., where satellite observations exist), there is a strong correspondence between regions of enhanced to fast (i.e., >5 m yr^{-1}) ice surface flow and disruption to englacial (internal) layering. This is most clearly demonstrated by the finding that ice flows in regions of disrupted internal layering at satellite-derived surface velocities, u, 436% greater than in regions where internal layering is undisrupted (Table 3), and by the predominance of disrupted layering over undisrupted layering at high ice velocities shown in Figure 4. These relationships also coincide with variations in subglacial roughness: RES bed echoes where $u > 5$ m yr^{-1} yield an average subglacial roughness 51% smoother than RES bed

Table 3. Lengths of RES Flight Tracks Displaying Undisrupted or Disrupted Internal Layers Corresponding With Regions of Slow (Source Region) Flow, Intermediate (Tributary) Flow, and Fast (Ice Stream) Flow, Defined by Satellite-Derived Surface Velocities for the Control Zone and by Balance Velocities for Both the Control Zone and the Entire Domain[a]

	Control Zone				Entire Domain	
	Flow Category Derived From u		Flow Category Derived From v		Flow Category Derived From v	
	Undisrupted	Disrupted	Undisrupted	Disrupted	Undisrupted	Disrupted
Source region (<5 m yr^{-1})	560	90	400	140	5140	3720
Tributary (5–100 m yr^{-1})	490	610	620	540	1360	3810
Ice stream (>100 m yr^{-1})	–	30	30	50	70	150
Totals	1050	730	1050	730	6570	7680

[a]RES flight track lengths given in kilometers. Here u denotes satellite-derived surface velocities and v denotes balance velocities. Undisrupted and disrupted denote layer class.

Table 4. Dimensionless Average Subglacial Roughness Values for Regions of Slow, Intermediate, and Fast Flow Speed, as Defined for Table 3[a]

	Control Zone		Entire Domain
	Flow Category Derived From u	Flow Category Derived From v	Flow Category Derived From v
Source region (<5 m yr^{-1})	0.184	0.138	0.096
Tributary (5–100 m yr^{-1})	0.094	0.114	0.109
Ice stream (>100 m yr^{-1})	0.040	0.094	0.092

[a]Slow flow is <5 m yr^{-1}, intermediate flow is 5–100 m yr^{-1}, and fast flow is >100 m yr^{-1}.

echoes in regions where $u < 5$ m yr^{-1} (Table 4), and the subglacial interface is typically smoother where faster ice flow is observed (Figure 5). These results are consistent with evidence presented elsewhere that disrupted (a.k.a. warped/distorted/buckled/scattered) internal layers [*Bell et al.*, 1998; *Fujita et al.*, 1999; *Jacobel et al.*, 1993, 1996; *Matsuoka et al.*, 2003; *Rippin et al.*, 2003b; *Siegert et al.*,

Figure 5. Scatterplots of subglacial roughness versus ice flow speeds, as represented by (a) satellite-derived ice-flow speeds, only available in the control zone; (b) balance velocities only in the control zone; and (c) balance velocities across the entire study domain. Subglacial roughnesses along flight tracks parallel to ice flow are plotted in gray; subglacial roughnesses along flight tracks orthogonal to ice flow are plotted in black.

2003] and smooth subglacial topography [*Siegert et al.*, 2005, 2004] are associated with ice streams and their tributaries within the polar ice sheets.

[24] The mechanisms responsible for the disruption to englacial stratigraphy and variations in subglacial roughness are still being debated. Most practitioners now concur that disruption to internal layering mostly occurs in response to past and present variations in the internal strain field across strain boundaries, exemplified by ice stream margins [*Bell et al.*, 1998; *Jacobel et al.*, 1993; *Siegert et al.*, 2003] and across enhanced-flow tributaries [*Jacobel et al.*, 1996; *Rippin et al.*, 2003b]. This may, in turn, be caused by changes in the basal boundary conditions at the onset of streaming [*Jacobel et al.*, 1993; *Ng and Conway*, 2004]. *Ng and Conway* [2004] have further demonstrated that the distortion of internal layers in Kamb Ice Stream (formerly Ice Stream C) may be a function of ice flow direction, and this may explain why in some regions of our analysis (notably grid NE of the SP; Figure 1b) we occasionally identify disrupted layering at right angles to undisrupted layering; in other words, there can be a primary axis of buckling orthogonal to which layers can appear to remain undisrupted.

[25] With respect to the correlation between ice streams, tributaries and variations in the spectral roughness of subglacial topography, it remains unclear as to whether variations in subglacial roughness precede ice sheet development and direct the initial development of ice streams and tributaries, or whether these flow features directly create the observed variations in subglacial roughness. It is possible that, as the ice sheet built up, ice streams and the tributaries feeding them preferentially developed along surfaces offering the least frictional resistance [*Siegert et al.*, 2005]. Certainly, however, once ice streams and tributaries are in place, subglacial erosion, especially aided by subglacial drainage, will play a large role in basal erosion, further smoothening the subglacial topography [*Hubbard et al.*, 2000; *Siegert et al.*, 2005]. Areas of smooth subglacial topography may also reflect regions of 'soft beds', where subglacial sediments are actively deforming beneath the ice base.

[26] Regardless of the mechanisms required to induce disruption of internal layers, or to dampen the spectral roughness of subglacial topography, the correspondence of these trends with contemporary ice streams and tributaries enables us to consider regions of disrupted internal layering and low subglacial roughness as indicators of the spatial and temporal extent of ice streams and enhanced-flow tributaries; this is especially valuable where neither satellite observations nor ground-based measurements of ice flow are available, such as in the region surrounding the SP. There-
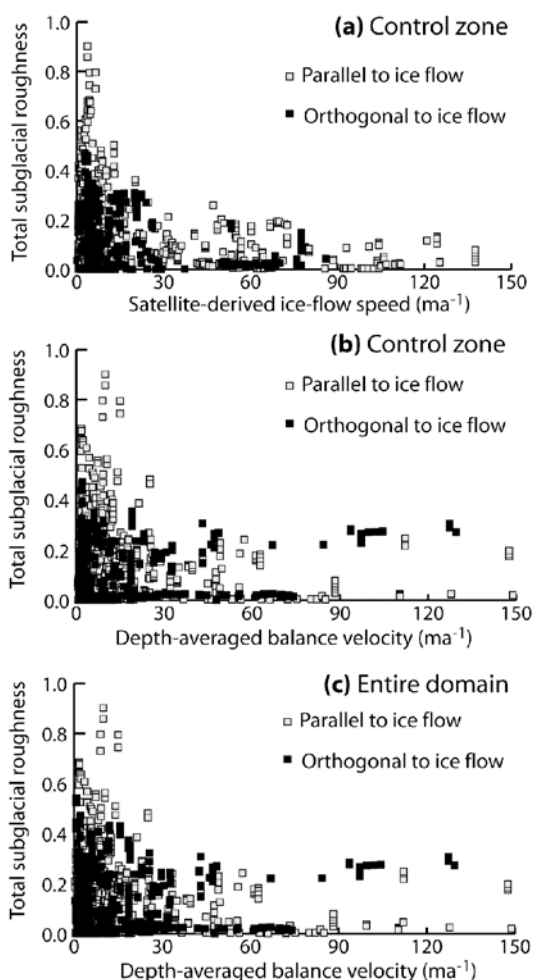
fore we can use our RES-derived parameters of englacial stratigraphic disruption and subglacial roughness to critique the current interpretation of ice flow fields around the SP and through the Support Force basin based on balance-flux models [*Bamber et al.*, 2000; *Le Brocq et al.*, 2006; *Wu and Jezek*, 2004].

[27] Our analysis of the RES data confirms the contention from balance-flux modeling that a tributary flowing into the SFIS originates in the vicinity of the SP. This is also consistent with GPS measurements of ice surface flow velocities made at the SP that yield ice flow of 9.99 ± 0.001 m yr^{-1} along the 39°50'34"W ± 0°.01 longitude line [*Schenewerk et al.*, 1994]. There can, therefore, be little doubt that a tributary connects this deep-interior region of East Antarctica to the FRIS via the SFIS. However, our analysis of the RES data suggests that the region of inception of this tributary is spread over a much wider area than is implied by balance-flux modeling (Figures 1b and 1d). This discrepancy between the balance-flux modeling and our RES interpretations of ice flow could be interpreted in three ways. First, if one assumes uncritically that balance-flux modeling represents the true ice flow pattern despite the reported low quality of surface elevation and ice thickness data in this region, then causes other than ice flow variability must be invoked to explain how internal layering has become disrupted and subglacial topography has become smoothened over such an extensive region around the SP. As flow variations are reportedly the dominant mechanism causing disruption to internal layering and variations in subglacial roughness [*Jacobel et al.*, 1993, 1996; *Ng and Conway*, 2004; *Rippin et al.*, 2003b; *Siegert et al.*, 2003; *Welch and Jacobel*, 2003], and there is a strong correspondence elsewhere between these parameters and variations in ice flow velocities[*Rippin et al.*, 2003b; *Siegert et al.*, 2003], this explanation seems unlikely. An alternative explanation is that the ice flow field may have altered over time, leaving a signature of disrupted internal layering (and perhaps smooth subglacial topography) where no tributary or ice-stream flow exists today. This is probably dependent upon the degree of topographic constraints to the flow field, which cannot be tested without further data; however, the extreme smoothness of subglacial topography beneath the downstream SFIS suggests that the SFIS, at least, has been very long-lived. Finally, if we assume that the RES-derived interpretation of the spatial extent of the tributary feeding the SFIS is correct, and that this represents a long-lived and relatively stable phenomenon, our analysis of the RES data over the Support Force basin and SP raises doubts about the validity of using steady state balance velocities as proxies for the depth-averaged ice flow field in the most central region of East Antarctica, at least until errors are reduced in the input data sets to the balance velocity models.

[28] Thus our analysis supports the contention that disrupted internal layers and smooth subglacial interfaces detected by RES can be used as indicators of tributary and/or ice stream flow. Applying this methodology to central Antarctica, our RES analysis supports the existence of a tributary network upstream of SFIS and FIS similar, but not identical, to that calculated by balance-flux modeling. Differences between RES-interpreted and balance-flux modeled ice flow patterns could be interpreted in terms of past or present changes in ice flow conditions, and raise concerns over the uncritical use of balance velocities as proxies for ice flow. Therefore RES provides a useful means of investigating ice flow in data-sparse regions of Antarctica, but more research is required to elucidate the mechanisms that are responsible for causing disruption to internal layering and bringing about variations in subglacial roughness.

5. Conclusions

[29] An interrogation of both modern and >30-year-old RES-derived data sets from the Support Force and Foundation Ice Stream drainage basins has shed new light on the ice flow pattern between interior East Antarctica and the Filchner-Ronne Ice Shelf. Our analysis has provided the first empirical confirmation that an organized flow network originates from within deep-interior East Antarctica, encompassing the region surrounding the South Pole, and connects that region with the Filchner-Ronne Ice Shelf via the Support Force Ice Stream. The contention that regions of fast (>100 m yr^{-1}) or enhanced ($5-100$ m yr^{-1}) ice flow are signified by disrupted internal layering and/or low subglacial roughness was validated against the available coverage of satellite-derived surface velocities within the Support Force and Foundation Ice Stream basins, and is also supported by similar studies undertaken elsewhere in Antarctica. The identification of disruptions to the englacial stratigraphy of ice layers and variations in subglacial roughness from RES data therefore constitutes a powerful methodology with which to delineate variations in ice flow configuration, in particular where other forms of evidence, such as those derived from satellite remote sensing, are sparse.

[30] We have used our RES-derived interpretation of the ice flow field through the Support Force basin to assess ice flow south of 86°S, the latitudinal limit of accurate satellite measurements of surface elevation. Although the results confirm the existence of enhanced flow beneath the South Pole, as previously indicated by balance-flux modeling, the RES data have yielded a more detailed understanding of the tributary's inception and spatial extent, which is spread over a much larger area around the pole than balance-flux modeling implies. The presence of this drainage feature from RES confirms that organized flow is prevalent between the South Pole and Filchner-Ronne Ice Shelf, and suggests that any applications reliant upon currently available balance velocities as proxies for ice flow in interior Antarctica should be interpreted with caution. Furthermore, it is evident that the Support Force Ice Stream, draining from interior East Antarctica, is essentially linked to the West Antarctic Ice Sheet through the Filchner-Ronne Ice Shelf; hence the stability of both the West and East Antarctic Ice Sheets may be rather more entwined than is normally implied.

References

Alley, R. B., and R. A. Bindschadler (Eds.) (2001), *The West Antarctic Ice Sheet: Behavior and Environment*, *Antarct. Res. Ser.*, vol. 77, AGU, Washington, D. C.

Bamber, J., and J. L. Gomez-Dans (2005), The accuracy of digital elevation models of the Antarctic continent, *Earth Planet. Sci. Lett.*, *237*(3–4), 516–523.

Bamber, J. L., D. G. Vaughan, and I. Joughin (2000), Widespread complex flow in the interior of the Antarctic ice sheet, *Science*, *287*(5456), 1248–1250.

Bell, R. E., D. D. Blankenship, C. A. Finn, D. L. Morse, T. A. Scambos, J. M. Brozena, and S. M. Hodge (1998), Influence of subglacial geology on the onset of a West Antarctic ice stream from aerogeophysical observations, *Nature*, *394*(6688), 58–62.

Bennett, M. R. (2003), Ice streams as the arteries of an ice sheet: Their mechanics, stability and significance, *Earth Sci. Rev.*, *61*(3–4), 309–339.

Berthier, E., B. Raup, and T. Scambos (2003), New velocity map and mass-balance estimate of Mertz Glacier, East Antarctica, derived from Landsat sequential imagery, *J. Glaciol.*, *49*, 503–511.

Bindschadler, R. (1998), Monitoring ice sheet behavior from space, *Rev. Geophys.*, *36*(1), 79–104.

Brigham, E. O. (1988), *The Fast Fourier Transform and Its Applications*, Prentice-Hall, Englewood Cliffs, N. J.

Budd, W. F., and R. C. Warner (1996), A computer scheme for rapid calculations of balance-flux distributions, *Ann. Glaciol.*, *23*, 21–27.

Davis, C. H., Y. Li, J. R. McConnell, M. M. Frey, and E. Hanna (2005), Snowfall-driven growth in East Antarctic Ice Sheet mitigates recent sea-level rise, *Science*, *308*(5730), 1898–1901.

Davis, M. B. (2001), Subglacial morphology and structural geology in the Southern Transantarctic Mountains from airborne geophysics, M. S. thesis, Univ. of Texas, Austin.

Drewry, D. J. (1983), *Antarctica: Glaciological and Geophysical Portfolio*, Scott Polar Res. Inst., Univ. of Cambridge, Cambridge, U. K.

Eisen, O., F. Wilhelms, U. Nixdorf, and H. Miller (2003), Revealing the nature of radar reflections in ice: DEP-based FDTD forward modeling, *Geophys. Res. Lett.*, *30*(5), 1218, doi:10.1029/2002GL016403.

Fujita, S., H. Maeno, S. Uratsuka, T. Furukawa, S. Mae, Y. Fujii, and O. Watanabe (1999), Nature of radio echo layering in the Antarctic ice sheet detected by a two-frequency experiment, *J. Geophys. Res.*, *104*(B6), 13,013–13,024.

Hubbard, B., M. J. Siegert, and D. McCarroll (2000), Spectral roughness of glaciated bedrock geomorphic surfaces: Implications for glacier sliding, *J. Geophys. Res.*, *105*(B9), 21,295–21,303.

Hughes, T. J. (1998), *Ice Sheets*, 343 pp., Oxford Univ. Press, New York.

Intergovernmental Panel on Climate Change (2001), *Climate Change 2001: The Scientific Basis*, edited by J. T. Houghton et al., Cambridge Univ. Press, New York.

Jacobel, R. W., A. M. Gades, D. L. Gottschling, S. M. Hodge, and D. L. Wright (1993), Interpretation of radar-detected internal layer folding in West Antarctic ice streams, *J. Glaciol.*, *39*, 528–537.

Jacobel, R. W., T. A. Scambos, C. F. Raymond, and A. M. Gades (1996), Changes in the configuration of ice stream flow from the West Antarctic Ice Sheet, *J. Geophys. Res.*, *101*(B3), 5499–5504.

Joughin, I., L. Gray, R. Bindschadler, S. Price, D. Morse, C. Hulbe, K. Mattar, and C. Werner (1999), Tributaries of West Antarctic ice streams revealed by RADARSAT interferometry, *Science*, *286*(5438), 283–286.

Joughin, I., J. L. Bamber, T. Scambos, S. Tulaczyk, M. Fahnestock, and D. R. Macayeal (2006), Integrating satellite observations with modelling: Basal shear stress of The Filchner-Ronne ice streams, Antarctica, *Philos. Trans. R. Soc., Ser. A*, *364*(1844), 1795–1814.

Lang, O., B. T. Rabus, and S. W. Dech (2004), Velocity map of the Thwaites Glacier catchment, *West Antarctica, J. Glaciol.*, *50*, 46–56.

Le Brocq, A. M., A. J. Payne, and M. J. Siegert (2006), West Antarctic balance calculations: Impact of flux-routing algorithm, smoothing and topography, *Comput. Geosci.*, *32*(10), 1780–1795.

Liu, H., K. C. Jezek, and B. Li (1999), Development of an Antarctic digital elevation model by integrating cartographic and remotely sensed data: A geographic information system based approach, *J. Geophys. Res.*, *104*(B10), 23,199–23,213.

Lythe, M. B., D. G. Vaughan, and the BEDMAP Consortium (2001), BEDMAP: A new ice thickness and subglacial topographic model of Antarctica, *J. Geophys. Res.*, *106*(B6), 11,335–11,351.

Matsuoka, K., T. Furukawa, S. Fujita, H. Maeno, S. Uratsuka, R. Naruse, and O. Watanabe (2003), Crystal orientation fabrics within the Antarctic ice sheet revealed by a multipolarization plane and dual-frequency radar survey, *J. Geophys. Res.*, *108*(B10), 2499, doi:10.1029/2003JB002425.

Matsuoka, K., S. Uratsuka, S. Fujita, and F. Nishio (2004), Ice-flow-induced scattering zone within the Antarctic ice sheet revealed by high-frequency airborne radar, *J. Glaciol.*, *50*, 382–388.

Miners, W. D., E. W. Wolff, J. C. Moore, R. Jacobel, and L. Hempel (2002), Modeling the radio echo reflections inside the ice sheet at Summit, Greenland, *J. Geophys. Res.*, *107*(B8), 2172, doi:10.1029/2001JB000535.

Ng, F., and H. Conway (2004), Fast-flow signature in the stagnated Kamb Ice Stream, West Antarctica, *Geology*, *32*(6), 481–484.

Rignot, E., and R. H. Thomas (2002), Mass balance of polar ice sheets, *Science*, *297*(5586), 1502–1506.

Rippin, D. M., J. L. Bamber, M. J. Siegert, D. G. Vaughan, and H. F. J. Corr (2003a), Basal topography and ice flow in the Bailey/Slessor region of East Antarctica, *J. Geophys. Res.*, *108*(F1), 6008, doi:10.1029/2003JF000039.

Rippin, D. M., M. J. Siegert, and J. L. Bamber (2003b), The englacial stratigraphy of Wilkes Land, East Antarctica, as revealed by internal radio-echo sounding layering, and its relationship with balance velocities, *Ann. Glaciol.*, *36*, 189–196.

Rose, K. E. (1978), Radio echo sounding studies of Marie Byrd Land, Antarctica, Ph.D. thesis, Univ. of Cambridge, Cambridge, U.K.

Rose, K. E. (1979), Characteristics of ice flow in Marie Byrd Land, Antarctica, *J. Glaciol.*, *24*, 63–74.

Schenewerk, M. S., J. R. MacKay, L. D. Hothem, and G. Shupe (1994), Determination of ice flow velocities at the South Pole using measurements from the global positioning system (GPS), research project report, Natl. Oceanic and Atmos. Admin., Silver Spring, Md. (Available at http://www.ngs.noaa.gov/GRD/GPS/Projects/SOUTH_POLE/south_pole.html)

Siegert, M. J. (1999), On the origin, nature and uses of Antarctic ice-sheet radio-echo layering, *Prog. Phys. Geogr.*, *23*(2), 159–179.

Siegert, M. J., A. J. Payne, and I. Joughin (2003), Spatial stability of Ice Stream D and its tributaries, West Antarctica, revealed by radio-echo sounding and interferometry, *Ann. Glaciol.*, *37*, 377–382.

Siegert, M. J., J. Taylor, A. J. Payne, and B. Hubbard (2004), Macro-scale bed roughness of the Siple Coast ice streams in West Antarctica, *Earth Surf. Processes Landforms*, *29*(13), 1591–1596.

Siegert, M. J., J. Taylor, and A. J. Payne (2005), Spectral roughness of subglacial topography and implications for former ice-sheet dynamics in East Antarctica, *Global Planet. Change*, *45*, 249–263.

Taylor, J., M. J. Siegert, A. J. Payne, and B. Hubbard (2004), Regional-scale bed roughness beneath ice masses: Measurement and analysis, *Comput. Geosci.*, *30*(8), 899–908.

Vaughan, D. G., J. L. Bamber, M. Giovinetto, J. Russell, and A. P. R. Cooper (1999), Reassessment of net surface mass balance in Antarctica, *J. Clim.*, *12*(4), 933–946.

Welch, B. C., and R. W. Jacobel (2003), Analysis of deep-penetrating radar surveys of West Antarctica, USITASE 2001, *Geophys. Res. Lett.*, *30*(8), 1444, doi:10.1029/2003GL017210.

Wu, X. L., and K. C. Jezek (2004), Antarctic ice-sheet balance velocities from merged point and vector data, *J. Glaciol.*, *50*, 219–230.

———————————

R. G. Bingham, British Antarctic Survey, Natural Environment Research Council, High Cross, Madingley Road, Cambridge CB3 0ET, UK. (rgbi@bas.ac.uk)

D. D. Blankenship and D. A. Young, Institute for Geophysics, John A. and Katherine G. Jackson School of Geosciences, University of Texas at Austin, 4412 Spicewood Springs Road, Austin, TX 78759, USA.

M. J. Siegert, Centre for Polar Observation and Modelling, School of GeoSciences, University of Edinburgh, Grant Institute, King's Buildings, West Mains Road, Edinburgh EH9 3JW, UK.